ACS APPLIED MATERIALS & INTERFACES

Research Article

www.acsami.org

Size-Exclusive Magnetic Graphene/Mesoporous Silica Composites with Titanium(IV)-Immobilized Pore Walls for Selective Enrichment of Endogenous Phosphorylated Peptides

Nianrong Sun,[†] Chunhui Deng,*[,†] Yan Li,*[,‡] and Xiangmin Zhang[†]

[†]Department of Chemistry and Institutes of Biomedical Sciences, Fudan University, Shanghai 200433, China

[‡]Pharmaceutical Analysis Department, School of Pharmacy, Fudan University, Shanghai 201203, China

Supporting Information

ABSTRACT: Developing an effective separation method is necessary for identifying low-abundant endogenous phosphorylated peptides with the removal of proteins. In this work, we prepared size-exclusive magnetic graphene/mesoporous silica composites with titanium(IV)-immobilized pore walls (denoted as Ti^{4+}-MGMSs) for capturing endogenous phosphorylated peptides for mass spectrometry analysis. The introduction of hydrophilic polydopamine simplified the synthetic process of Ti^{4+}-MGMSs, and the ordered mesoporous channels are beneficial to the trapping of endogenous phosphopeptides while large-size proteins are excluded. Furthermore, the magnetic performance greatly simplifies the entire process of enrichment. With all of the advances, the novel Ti^{4+}-MGMSs present high enrichment efficiency either from the low concentration of β-casein tryptic digest (0.5 fmol/μL) or the mixture of β-casein tryptic digest and α-casein (or plus bovine serum albumin, with a mass ratio up to 1:500). Besides, Ti^{4+}-MGMSs have also been successfully applied to enrich endogenous phosphorylated peptides from human serum and human saliva.

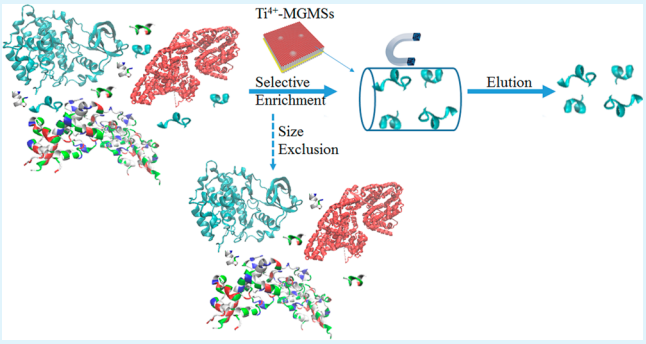

KEYWORDS: *magnetic graphene, mesoporous silica, size-exclusive, titanium, endogenous phosphorylated peptides*

1. INTRODUCTION

Peptidome, which is referred as the peptides that expressed in any cell, tissue, or biofluid at any given time, has become more and more attention-grabbing because of its potential in the discovery of biomarkers associated with human diseases and the simplicity of sample preparation (existing in the native state). Immense amounts of concrete research have repeatedly demonstrated that the peptides in the tissues or body fluid can provide useful information for clinical diagnosis.[1−5] Over these years, although mass spectrometry (MS) has been widely used in the signal detection of peptides, it remains difficult to analyze the peptides from complex biological samples because of the extremely high dynamic range of complex biological samples.

Conventional approaches for enriching peptides from complex biological samples are solid-phase extraction[6,7] and centrifugal ultrafiltration.[2,3] However, according to the reports by Villanueva's group,[8] solid-phase extraction showed low efficiency for the selective enrichment of peptide against protein. Although centrifugal ultrafiltration based on a size-exclusion mechanism revealed high enrichment selectivity to low-molecular-weight peptidome,[9−11] it presents low enrichment efficiency especially for blood samples.[12] In recent years, owing to the outstanding features of large surface area, stability, and uniform mesochannels, a large number of innovative techniques based on ordered mesoporous materials have been established and show excellent selective enrichment capability for peptides in peptidome research.[13−18] Recently, functionalized magnetic graphene/mesoporous materials have also been designed and synthesized for the selective enrichment of endogenous peptides in peptidome research,[19] which has simplified the whole enrichment process significantly. In spite of the fact that great progress for peptidome analysis has been made, modified endogenous peptides, especially endogenous phosphorylated peptides that play a significant role, are less reported to date. Besides the low ionization efficiency and abundance of endogenous phosphorylated peptide in complex biological samples, suppression from highly abundant proteins and nonphosphorylated peptides contained in complex biological samples is also an important reason. Therefore, it is essential to develop a suitable method with high selectivity and protein exclusion ability to purify endogenous phosphorylated peptides for peptidome analysis.

Received: April 29, 2014
Accepted: July 1, 2014
Published: July 1, 2014

dx.doi.org/10.1021/am502529a | ACS Appl. Mater. Interfaces 2014, 6, 11799−11804

Scheme 1. Workflow of the Synthesis of Ti^{4+}-MGMSs

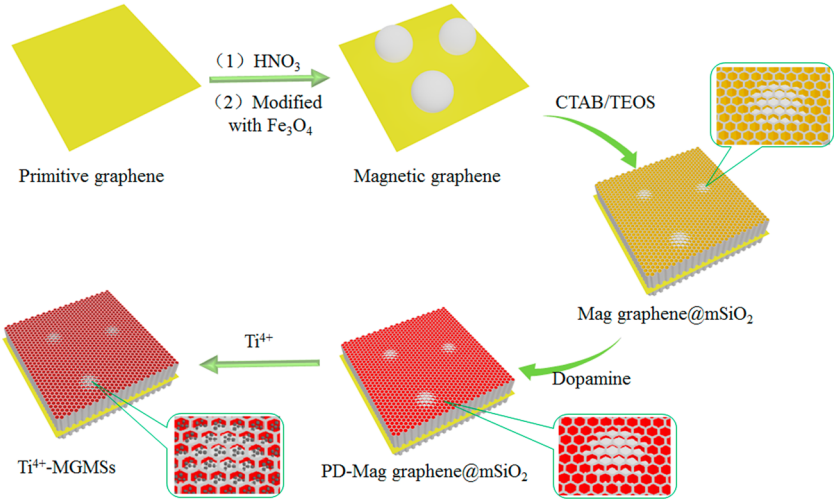

More recently, in our group, a novel IMAC material was designed, synthesized with polydopamine coated on the surface of graphene, and functionalized with titanium ions (denoted as Ti^{4+}-G@PD) for phosphoproteome research. The grafting layer of polydopamine decoration would provide enhanced hydrophilicity and biocompatibility. On the other hand, the high surface area of graphene would offer a higher capacity for loading dopamine and enhance the amount of immobilized titanium ions, which would result in a larger capacity of phosphopeptide binding.[20] Herein, we further developed polydopaime-coated magnetic graphene/mesoporous silica composites with titanium(IV)-immobilized pore walls (denoted as Ti^{4+}-MGMSs) to selectively capture low-abundant endogenous phosphorylated peptides for peptidome analysis. By virtue of all of the advantages of polydopamine, graphene, mesopore, magnetic property, and the specific interaction between titanium and phosphate groups, the novel materials exhibited a good enrichment performance from digestion of a standard phosphoprotein β-casein as well as the mixture of the β-casein digest and interfering proteins [α-casein and bovine serum albumin (BSA)]. Besides, Ti^{4+}-MGMSs were also successfully employed to enrich endogenous phosphorylated peptides from human serum and human saliva.

2. RESULTS AND DISCUSSION

Synthesis and Characterization of Ti^{4+}-MGMSs. The synthetic procedure is shown in Scheme 1. Briefly, first, pristine graphene slices were treated with a hot concentrated nitric acid solution to activate the surface of graphene (which was filled with hydroxyl and carboxyl). Second, magnetic graphene composites were prepared via a solvothermal reaction, and then a layer of mesoporous silica was coated onto the surface of activated graphene through a surfactant (cetyltrimethylammonium bromide, CTAB) involving a sol–gel process utilizing tetraethyl orthosilicate (TEOS) as the silicon precursor. Afterward, magnetic graphene@$mSiO_2$ was mixed with dopamine under mechanical agitation for 15 min to the acquire polydopamine-modified magnetic graphene/mesoporous silica composites (PD-Mag graphene@$mSiO_2$ composites). Finally, PD-Mag graphene@$mSiO_2$ composites were incubated in a solution of $Ti(SO_4)_2$ for 2 h to immobilize Ti^{4+}. The final products were collected by magnetic action and washed with water and ethyl alcohol in order.

The morphology of Ti^{4+}-MGMSs was characterized by scanning electron microscopy (SEM) and transmission electron microscopy (TEM). The SEM image shows that the obtained magnetic particles, which have rough uniform spherical morphology, are scattered on graphene with a rough surface (Figure 1a). The TEM image viewed from Figure 1b indicates

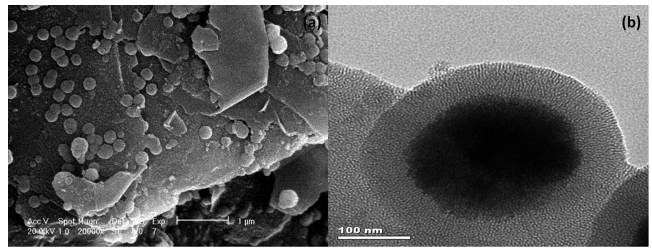

Figure 1. SEM (a) and TEM (b) images of Ti^{4+}-MGMSs.

the existence of a porous structure of the composites and a mean size of the Fe_3O_4 particles of about 170 nm. In addition, as shown in Figure S1 in the Supporting Information (SI), Ti^{4+}-MGMSs can be dispersed in water and magnetically separated.

The wide-angle X-ray diffraction measurement of Ti^{4+}-MGMSs was also investigated. As shown in Figure S1 in the SI, a strong diffraction peak at around 26° can be observed and is due to the large number of graphitic layers in the composites. At the same time, the diffraction peaks of (220), (311), (400), and (440) would be indexed as the characteristic peaks of Fe_3O_4 (Figure S2 in the SI). From Figure 2, obviously, the mesoporous structure of Ti^{4+}-MGMSs was retained after modification of polydopamine. The typical IV isotherm with a hysteresis loop of mesoporous materials defined by IUPAC was acquired. The sudden increase of P/P_0 from 0.3 to 0.7 indicates the uniform pore-size distribution of Ti^{4+}-MGMSs. The Brunauer–Emmett–Teller surface area of Ti^{4+}-MGMSs is 224.6 m^2/g, and from the inset of Figure 2, the pore size was estimated to be 2.17 nm, which is suitable for capturing small-molecule targets while excluding proteins with large molecular weight.[13,21] In the meantime, the pore size of the magnetic graphene@$mSiO_2$ material was estimated to be 3.98 nm (Figure S3 in the SI) by the same method, which means that the pore size becomes smaller after modification of polydop-

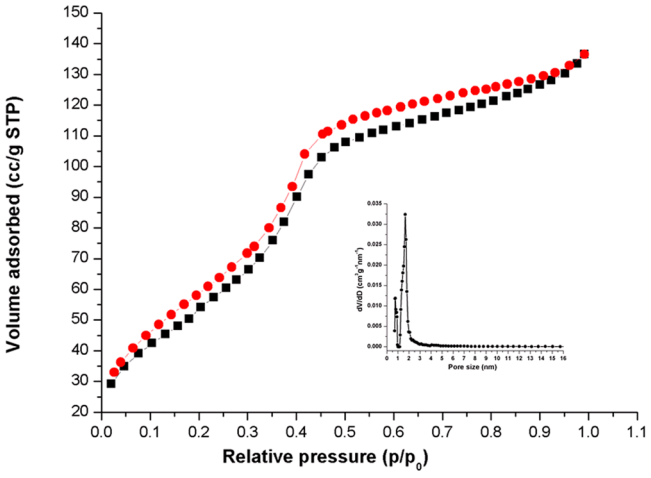

Figure 2. Nitrogen sorption isotherms and pore-size distribution (inset) of Ti^{4+}-MGMSs.

amine; namely, polydopamine was coated on the inner wall of the pore successfully.

To further verify the successful modification of polydopamine and the successful grafting of titanium, the obtained Ti^{4+}-MGMSs were further examined by an energy-dispersive X-ray detector. As depicted in Figure S4a in the SI, the peaks of carbon, nitrogen, oxygen, silicon, titanium, and iron were observed, which indicates that polydopamine has been modified and titanium has been successfully grated on the magnetic graphene mesoporous silica composites. The specific compositions of the elements are listed in Figure S4b in the SI. The atom and weight percentages of titanium are estimated to be 0.94% and 1.92%, respectively.

Application of Ti^{4+}-MGMSs to Phosphopeptide Enrichment in Peptidome Research. At first, considering the specific interaction between titanium ions and phosphorylated peptide, the Ti^{4+}-MGMSs were used to extract phosphorylated peptide released from β-casein (with a small quantity of α-casein). After enrichment with Ti^{4+}-MGMSs, 14 phosphorylated peptides can be observed along with an obviously increased signal-to-noise ratio (S/N). It is worth mentioning that some phosphorylated peptides assigned to α-casein could also be detected because a small quantity of α-casein existed in β-casein. The detailed information on phosphorylated peptides is shown in Table S1 in the SI. Moreover, the identities of part of the phosphopeptides from a β-casein digest solution are further confirmed by matrix-assisted laser desorption ionization (MALDI) MS/MS. From Figure S5a–d in the SI, the four peaks observed can be assigned to dephosphorylated fragments of a phosphorylated peptide due to the loss of H_3PO_4. In a word, the results certify that Ti^{4+}-MGMSs can be successfully employed for capturing phosphorylated peptides.

The detection limit of Ti^{4+}-MGMSs was further explored by confecting a series of concentration gradients of a β-casein digest solution. As shown in Figure 3, two MS signals of phosphopeptides with S/N over 10 could still be observed after enrichment in a β-casein digest solution with an ultralow concentration of 0.5 fmol/μL. The low detection limit of the novel materials could be attributed to the large surface area of Ti^{4+}-MGMSs and the specific interaction between titanium ions and phosphorylated peptides. In addition, because of the existence of magnetic particles, quite rapid magnetic separation of Ti^{4+}-MGMSs could be obtained with the aid of an external magnetic field, which made the whole enrichment process significantly simplified.

Furthermore, standard proteins were employed to study the size-exclusion effect of Ti^{4+}-MGMSs with uniform mesoporous structure. In the first place, the size-exclusive performance of Ti^{4+}-MGMSs was investigated with a mixture of β-casein tryptic digest and undigested α-casein as the interfering protein. Figure S6 in the SI demonstrates the MS spectra of β-casein tryptic

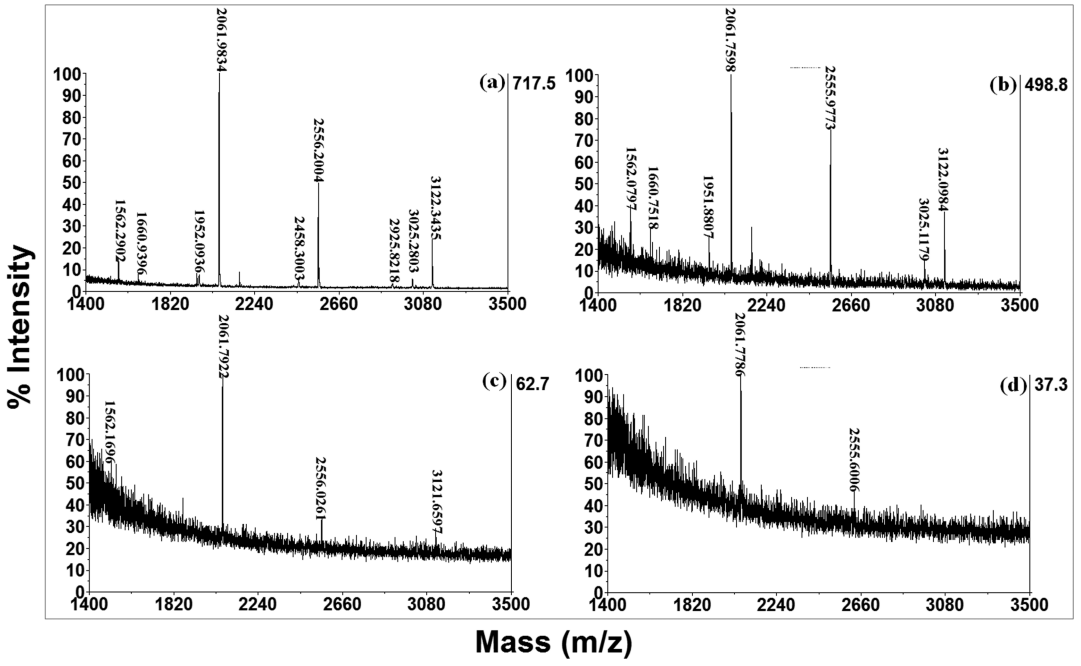

Figure 3. MALDI-TOF-MS spectra of different concentrations of the β-casein tryptic digests after enrichment by Ti^{4+}-MGMSs: (a) 20 fmol/μL; (b) 2 fmol/μL; (c) 1 fmol/μL; (d) 0.5 fmol/μL.

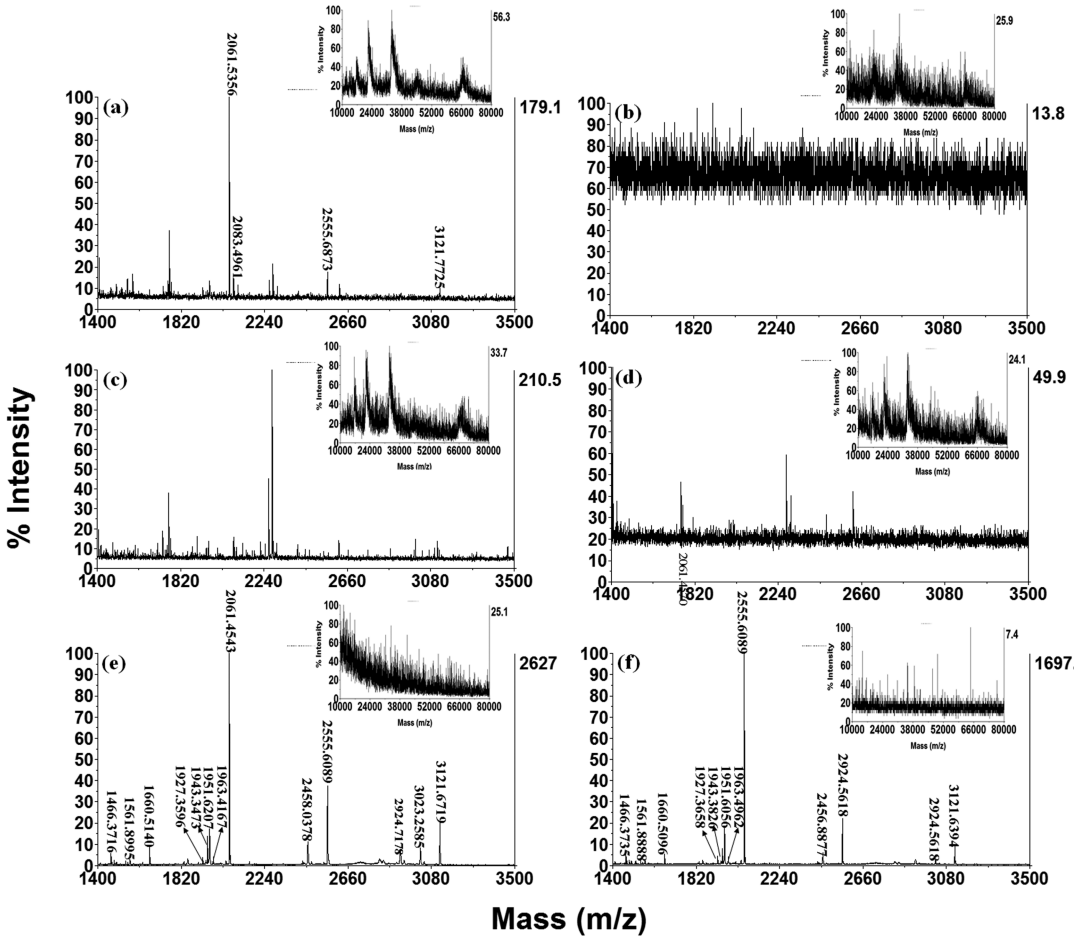

Figure 4. MS spectra of a mixture of β-casein tryptic digests (5 μg/μL,1 μL), phosphorylated protein (α-casein; molecular weight = 25 kD), and nonphosphorylated protein (BSA; molecular weight = 66 kD) with different mass ratios: (a and b) without any treatment; (c and d) supernatant after enrichment by Ti^{4+}-MGMSs; (e and f) eluent after enrichment by Ti^{4+}-MGMSs. The mass ratios of β-casein/α-casein/BSA are 1:100:100 (a, c, and e) and 1:500:500 (b, d, and f). Analysis of the proteins was performed in linear TOF detection modes.

digest and α-casein at different mass ratios without treatment (Figure S6a–d in the SI) and after enrichment (Figure S6e–h in the SI) by Ti^{4+}-MGMSs. From Figure S6a in the SI, MS signals of phosphorylated peptides were observed with a low MS signal even in the absence of α-casein, and when the mass ratio was up to 1:500, the signals of phosphorylated peptides were totally submerged (Figure S6d in the SI). Nonetheless, according to the corresponding MS spectra of β-casein tryptic digest/α-casein (1:0; 1:50; 1:100, and 1:500) enriched by Ti^{4+}-MGMSs (Figure S6e–h in the SI), more than 10 phosphorylated peptides were detected in each figure. Among those peptides, three peaks at m/z 2061, 2556, and 3122 (main characteristic peaks released from β-casein) can be clearly observed with very high S/N. Meanwhile, for comparison, titanium-ion-modified magnetic graphene (denoted as Ti^{4+}-Mag G@PD) was synthesized to treat a mixture of β-casein tryptic digests and α-casein protein with a mass ratio at 1:500. From Figure S7a in the SI, 15 phosphorylated peptides can be detected after enrichment with Ti^{4+}-MGMSs. Only 7 phosphorylated peptides with lower MS signals were detected (Figure S7b in the SI) after enrichment with Ti^{4+}-Mag G@PD, confirming the size-exclusive selective enrichment of mesoporous silica.

In the second place, because massive proteins were contained in practical biological samples, further efforts were made to utilize a more complicated sample to prove the size-exclusive ability of the obtained materials. A mixture of β-casein tryptic digest, undigested α-casein, and BSA was used to evaluate the performance of Ti^{4+}-MGMSs for the selective trapping of phosphorylated peptides. When there was no protein in the β-casein tryptic digest (5 μg in 200 μL of loading buffer), 14 phosphorylated peptides were detected after treatment with Ti^{4+}-MGMSs (Figure S8e in the SI), while only 8 phosphorylated peptides with weak signal intensities were detected by direct MS analysis (Figure S8a in the SI). When the mass ratio of β-casein tryptic digest/α-casein/BSA was 1:50:50, before treatment with mesoporous composites, except five peaks of phosphorylated peptides (Figure S8b in the SI), the protein peaks (inset in Figure S8b in the SI) were simultaneously detected. However, after treatment with Ti^{4+}-MGMSs, only the peaks of proteins were observed in the supernatant (Figure S8d in the SI), while 13 phosphorylated peptides released from the adsorbent (Figure S8f in the SI) were observed with significantly increased MS signals. It is also worth mentioning that no protein peaks could be detected in the eluent (inset in Figure S8f in the SI). The results above demonstrated that small phosphorylated peptides could be readily enriched by Ti^{4+}-MGMSs, whereas proteins were size-excluded by the mesopores and remained in the supernatant ascribed to the large size. Even when the mass ratio of β-casein tryptic digest/α-casein/BSA soared to 1:100:100 and 1:500:500, over 10 phosphorylated peptides' signal (Figure

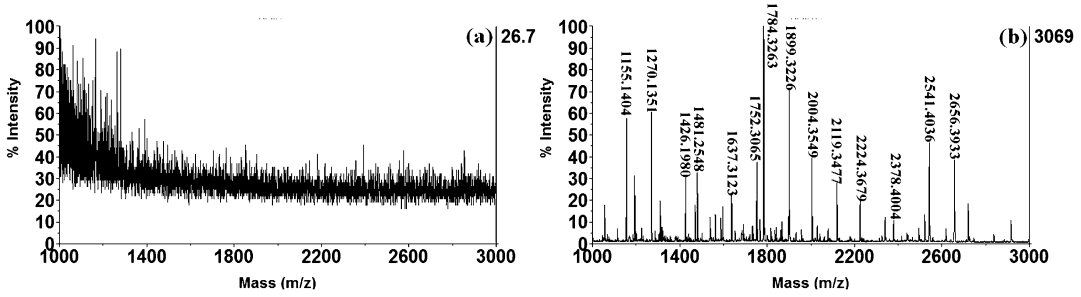

Figure 5. MALDI-TOF-MS spectra of endogenous phosphorylated peptides in pristine human saliva diluted by a factor of about 4: (a) without and (b) after enrichment with Ti^{4+}-MGMSs.

4e,f) could be obtained without any protein signal (which was discarded in the supernatant; inset in Figure 4c,d), which hinted at the importance of mesopores in Ti^{4+}-MGMSs for the size-selective enrichment of target molecules from protein-rich biosamples. Meanwhile, all of the above results further suggested that the highly ordered open and uniform mesopores of Ti^{4+}-PMGMs had an immense application prospect in endogenous phosphorylated peptide profiling for peptidome research.

Encouraged by the above results, further experiments with healthy human serum as the sample were conducted to confirm the enrichment efficiency of Ti^{4+}-MGMSs for endogenous phosphorylated peptides. As revealed in Figure S9 in the SI, no signal was shown when human serum (which was diluted 100 times) was directly analyzed by MS. After enriched by Ti^{4+}-MGMSs, four peaks at m/z 1389.609, 1460.605, 1545.698, and 1616.889 assigned to phosphorylated peptides were detected. The particular information on endogenous phosphorylated peptides is exhibited in Table S2 in the SI.

Human saliva is a colorless complex liquid that has a myriad of functions including lubricating oral mucosa, dissolving food, and facilitating swallowing, contains amylase and lysozyme that can help digestion, and has an antiseptic effect. Scientists believe that changes in saliva are indicative of the healthiness of the body,[22] and the diagnosis of diseases using human saliva[23,24] will be explored by more and more laboratories. Here, we chose human saliva as real samples to further apply our materials to analyze endogenous phosphorylated peptides. As shown in Figure 5b, enriched by Ti^{4+}-MGMSs, a total of 14 endogenous phosphorylated peptides were detected. Each of the endogenous phosphorylated peptides from human saliva was further identified by MALDI MS/MS. The spectra are shown in Figure S10 in the SI, and every observed peak can be assigned to dephosphorylated fragments of phosphorylated peptide by reason for the loss of H_3PO_4.

All of the above results indicated that Ti^{4+}-MGMSs owned great capability of fast enrichment for endogenous phosphorylated peptides, which ought to be due to its combined advantages, including the special interaction between Ti^{4+} and phosphorylated peptides, large surface area, size-exclusion effect of mesopores, and the existence of magnetic particles. In short, the remarkable selective enrichment ability of Ti^{4+}-MGMSs makes it a promising candidate for effectively enriching and separating endogenous phosphopeptides from real complex biological samples for peptidome research.

3. CONCLUSIONS

In this study, Ti^{4+}-MGMSs were successfully synthesized and applied to capture endogenous phosphopeptides. The introduction of hydrophilic polydopamine simplified the synthetic process of Ti^{4+}-MGMSs compared with previously reported methods.[14] Meanwhile, after modification with hydrophilic polydopamine, the ordered mesoporous channels still exist, which is beneficial to the trapping of endogenous phosphopeptides while large-size proteins are excluded. Furthermore, the magnetic performance greatly simplifies the entire process of enrichment. With all of the advantages, novel Ti^{4+}-MGMSs present high enrichment efficiency from either the low concentration of β-casein tryptic digest (0.5 fmol/μL) or a mixture of β-casein tryptic digest and α-casein (or plus BSA, even a mass ratio up to 1:500). Moreover, Ti^{4+}-MGMSs were successfully used to enrich endogenous phosphopeptides from human serum and human saliva. On the basis of the above results, it could be estimated that novel Ti^{4+}-MGMSs had broad application prospects for the selective enrichment of endogenous phosphopeptides in peptidome research.

■ ASSOCIATED CONTENT

Supporting Information

Experimental methods and additional data of Ti^{4+}-MGMSs and their performance in phosphopeptide enrichment. This material is available free of charge via the Internet at http://pubs.acs.org.

■ AUTHOR INFORMATION

Corresponding Authors

*E-mail: chdeng@fudan.edu.cn. Fax: +86-21-65641740.
*E-mail: yanli@fudan.edu.cn.

Notes

The authors declare no competing financial interest.

■ ACKNOWLEDGMENTS

This work was supported by the 973 Project (2013CB911201, 2012CB910602), the 863 Project (2012AA020202), and the National Natural Science Foundation of China (21075022, 20875017, and 21105016).

■ REFERENCES

(1) Schulte, I.; Tammen, H.; Selle, H.; Schulz-Knappe, P. Peptides in Body Fluids and Tissues as Markers of Disease. *Expert Rev. Mol. Diagn.* **2005**, *5*, 145−157.

(2) Diamandis, E. P. Peptidomics for Cancer Dignosis: Present and Future. *J. Proteome Res.* **2006**, *5*, 2079−2082.

(3) Petricoin, E. F.; Belluco, C.; Araujo, R. P.; Liotta, L. A. The Blood Peptidome: a Higher Dimension of Information Content for Cancer Biomarker Discovery. *Nat. Rev. Cancer* **2006**, *6*, 961−967.

(4) Petricoin, E. F.; Ardekani, A. M.; Hitt, B. A.; Levine, P. J.; Fusaro, V. A.; Steinberg, S. M.; Mills, G. B.; Simone, C.; Fishman, D. A.; Kohn, E. C.; Liotta, L. A. Use of Proteomic Patterns in Serum to Identify Ovarian Cancer. *Lancet* **2002**, *359*, 572−577.

(5) Villanueva, J.; Shaffer, D. R.; Philip, J.; Chaparro, C. A.; Erdjument-Bromage, H.; Olshen, A. B.; Fleisher, M.; Lilja, H.; Brogi, E.; Boyd, J.; Sanchez-Carbayo, M.; Holland, E. C.; Cordon-Cardo, C.; Scher, H. I.; Tempst, P. Differential Exoprotease Activities Confer Tumor-Specific Serum Peptidome Patterns. *J. Clin. Invest.* **2006**, *116*, 271−284.
(6) Rai, A. J.; Gelfand, C. A.; Haywood, B. C.; Warunek, D. J.; Yi, J.; Schuchard, M. D.; Mehigh, R. J.; Cockrill, S. L.; Scott, G. B.; Tammen, H.; Schulz-Knappe, P.; Speicher, D. W.; Mehigh, S. L.; Cockrill, G. B.; Scott, H.; Tammen, P.; Schulz-Knappe, D. W.; Vitzthum, F.; Haab, B. B.; Siest, G.; Chan, D. W. HUPO Plasma Proteome Project Specimen Collection and Handling: Towards the Standardization of Parameters for Plasma Proteome Samples. *Proteomics* **2005**, *5*, 3262−3277.
(7) Hsieh, S. Y.; Chen, R. K.; Pan, Y. H.; Lee, H. L. Systematical Evaluation of the Effects of Sample Collection Procedures on Low-Molecular-Weight Serum/Plasma Proteome Profiling. *Proteomics* **2006**, *6*, 3189−3198.
(8) Villanueva, J.; Philip, J.; Entenberg, D.; Chaparro, C. A.; Tanwar, M. K.; Holland, E. C.; Tempst, P. Serum Peptide Profiling by Magnetic Particle-Assisted, Automated Sample Processing and MALDI-TOF Mass Spectrometry. *Anal. Chem.* **2004**, *76*, 1560−1570.
(9) Johnson, K. L.; Mason, C. J.; Muddiman, D. C.; Eckel, J. E. Analysis of the Low Molecular Weight Fraction of Serum by LC-dual ESI-FT-ICR Mass Spectrometry: Precision of Retention Time, Mass, and Ion Abundance. *Anal. Chem.* **2004**, *76*, 5097−5103.
(10) Yuan, X.; Desiderio, D. M. Human Cerebrospinal Fluid Peptidomics. *J. Mass Spectrom.* **2005**, *40*, 176−181.
(11) Zheng, X. Y.; Baker, H.; Hancock, W. S. Analysis of the Low Molecular Weight Serum Peptidome Using Ultrafiltration and a Hybrid Ion Trap-Fourier Transform Mass Spectrometer. *J. Chromatogr. A* **2006**, *1120*, 173−184.
(12) Aristoteli, L. P.; Molloy, M. P.; Baker, M. S. Evaluation of Endogenous Plasma Peptide Extraction Methods for Mass Spectrometric Biomarker Discovery. *J. Proteome Res.* **2007**, *6*, 571−581.
(13) Yin, P.; Wang, Y. H.; Li, Y.; Deng, C. H.; Zhang, X. M.; Yang, P. Y. Preparation of Sandwich-Structured Graphene/Mesoporous Silica Composites with C8-Modified Pore Wall for Highly Efficient Selective Enrichment of Endogenous Peptides for Mass Spectrometry Analysis. *Proteomics* **2012**, *12*, 2784−2791.
(14) Hu, L. H.; Zhou, H. J.; Li, Y. H.; Sun, S. T.; Guo, L. H.; Ye, M. L.; Tian, X. F.; Gu, J. R.; Yang, S. L.; Zou, H. F. Profiling of Endogenous Serum Phosphorylated Peptides by Titanium (IV) Immobilized Mesoporous Silica Particles Enrichment and MALDI-TOFMS Detection. *Anal. Chem.* **2009**, *81*, 94−104.
(15) Qin, H. Q.; Gao, P.; Wang, F. J.; Zhao, L.; Zhu, J.; Wang, A. Q.; Zhang, T.; Wu, R. A.; Zou, H. F. Highly Efficient Extraction of Serum Peptides by Ordered Mesoporous Carbon. *Angew. Chem., Int. Ed.* **2011**, *50*, 12218−12221.
(16) Qin, H. Q.; Wang, F. J.; Wang, P. Y.; Zhao, L.; Zhu, J.; Yang, Q. H.; Wu, R. A.; Ye, M. L.; Zou, H. F. Phosphoric Acid Functionalized Mesoporous Organo-Silica (EPO) as the Adsorbent for in Situ Enrichment and Isotope Labeling of Endogenous Phosphopeptides. *Chem. Commun.* **2012**, *48*, 961−963.
(17) Zhu, G. T.; Li, X. S.; Gao, Q.; Zhao, N. W.; Yuan, B. F.; Feng, Y. Q. Pseudomorphic Synthesis of Monodisperse Magnetic Mesoporous Silica Microspheres for Selective Enrichment of Endogenous Peptides. *J. Chromatogr. A* **2012**, *1224*, 11−18.
(18) Liu, S. S.; Chen, H. M.; Lu, X. H.; Deng, C. H.; Zhang, X. M.; Yang, P. Y. Facile Synthesis of Copper(II) Immobilized on Magnetic Mesoporous Silica Microspheres for Selective Enrichment of Peptides for Mass Spectrometry Analysis. *Angew. Chem., Int. Ed.* **2010**, *49*, 7557−7561.
(19) Yin, P.; Sun, N. R.; Deng, C. H.; Li, Y.; Zhang, X. M.; Yang, P. Y. Facile Preparation of Magnetic Graphene Double-Sided Mesoporous Composites for the Selective Enrichment and Analysis of Endogenous Peptides. *Proteomics* **2013**, *13*, 2243−2250.
(20) Yan, Y. H.; Zheng, Z. F.; Deng, C. H.; Li, Y.; Zhang, X. M.; Yang, P. Y. Hydrophilic Polydopamine-Coated Graphene for Metal Ion Immobilization as a Novel Immobilized Metal Ion Affinity Chromatography Platform for Phosphoproteome Analysis. *Anal. Chem.* **2013**, *85*, 8483−8487.
(21) Sun, N. R.; Deng, C. H.; Li, Y.; Zhang, X. M. Highly Selective Enrichment of N-Linked Glycan by Carbon Functionalized Ordered Graphene/Mesoporous Silica Composites. *Anal. Chem.* **2014**, *86*, 2246−2250.
(22) Iorgulescu, G. Saliva Between Normal and Pathological. Important Factors in Determining Systemic and Oral Health. *J. Med. Life* **2009**, *2*, 303−307.
(23) Dodds, M. W.; Johnson, D. A.; Yeh, C. K. Health Benefits of Saliva: A Review. *J. Dent.* **2005**, *33*, 223−233.
(24) Lee, Y. H.; Wong, D. T. Saliva: An Emerging Biofluid for Early Detection of Diseases. *Am. J. Dent.* **2009**, *22*, 241−248.